Numerical Simulation of Ram Extrusion Processes of Short Fiber-Reinforced Fresh Cementitious Composite

Xiangming Zhou[1], and Zongjin Li[2]

Abstract: A series of ram extrusion tests are carried out on short fiber-reinforced, semi-solid, fresh cementitious composite. An elasto-viscoplastic constitutive model is proposed for the extrudable fresh cementitious composite, which features the associative flow rule, nonlinear strain rate-hardening law and von Mises yield criterion. The constitutive model is then implemented into the ANSYS/LS-DYNA explicit finite element code. Various ram extrusion processes of the fresh cementitious composite are simulated. It has been found that the predicted extrusion load versus imposed displacement data agree well with experimental results. The fresh paste flow, through the die entry and the die-land, is then interpreted in light of the evolution of deformation and distribution of state variables, mainly based on numerical results and ram extrusion mechanism. The effects of extrusion ratio and extrusion velocity on extrusion load are also investigated based on mechanical properties of the fresh cementitious composite. The study indicates that the numerical procedure established, together with the constitutive model proposed, is applicable for describing ram extrusion of short fiber-reinforced fresh cementitious composite, which might provide a numerical rheometric tool from which ram extrusion of elasto-viscoplastic paste-like materials can be examined and quantified.

Keywords: Elasto-viscoplastic; Constitutive model; Rheology; Strain rate; Fiber-reinforced; Fresh cementitious composite; Extrusion; LS-DYNA

1 Lecturer in Civil Engineering Design (Contact author), School of Engineering & Design, Brunel University, Kingston Lane, Uxbridge, Middlesex, UB8 3PH, United Kingdom, Tel: 44 189 526 6670, Fax: 44 189 525 6392, E-mail: Xiangming.Zhou@brunel.ac.uk

2 Professor, Department of Civil and Environmental Engineering, The Hong Kong University of Science and Technology, Clear Water Bay, Kowloon, Hong Kong, Tel: 852 2358 8751, Fax: 852 2358 1534, E-mail: zongjin@ust.hk

1. INTRODUCTION

Extrusion is a typical material processing technology for manufacturing semi-solid paste-like products throughout mechanical, chemical, ceramic, food and pharmaceutical industries. In the last two decades, this technique has been transferred to concrete industry as an economical, efficient and environmental-friendly manufacturing method for short fiber-reinforced cement-based construction materials and products (Shao et al. 1995; Shao and Shah 1997; Aldea et al. 1998; Li and Mu 1998; Li et al. 1999; Li et al 2001; Peled and Shah 2003; Li et al 2004). Comparing with traditional concrete casting method, extrusion technique can significantly improve mechanical properties of the final products through high shear and high compression processing environment within an extruder (Shao et al. 1995; Peled and Shah 2003). In practice, there are mainly two different extrusion methods: the continuous screw-driven method (screw extrusion) and the intermittent piston-driven method (ram extrusion). The screw-driven method allows continuous production. However, it is not generally suitable for small batch runs because of difficulties in cleaning the extruder (Aydin

et al. 2000). It may not even be possible for some materials, such as metal-alloys, due to limitations in rheology. On the other hand, ram extrusion is favored for short runs and accurate dimensional control (Aydin et al. 2000). In this method, a piston drives highly viscous, semi-solid fresh paste to flow through a die entrance and then a die-land, thereby reducing the cross-sectional area of the paste and shaping it as desired. The axisymmetric ram extrusion with a circular die entry, as shown in Figure 1, is a simple but effective method for tailoring mix proportion for extrudable fiber-reinforced cementitious composite (Srinivasan et al. 1999; Zhou and Li 2005a). The most widely used model for analyzing this type of ram extrusion data is based on a relationship known as the Benbow and Bridgwater equation (Benbow and Bridgwater 1993):

$$P = P_{ent} + P_{land} = 2\ln(\frac{D_0}{D})(\sigma_0^{'} + \alpha V_p^j) + \frac{4L}{D}(\tau_0^{'} + \beta V_p^q) \qquad (1\text{-}1)$$

(Place Fig. 1 here)

where, as shown in Fig. 1, P is the overall pressure drop; the first term of the right hand side of Eq. 1-1 is the die entry pressure drop, P_{ent}, representing that a plastic flow dominates at the die entry; the second term of the right hand side of Eq. 1-1 is the die-land pressure drop, P_{land}, representing a slip flow in the die-land; D_0 is the barrel diameter; D is the die-land diameter; L is the die-land length; V_p is the mean paste flow velocity in the die-land; $\sigma_0^{'}$ is the initial die entry yield stress when the paste velocity approaches zero; α is the die entry yield stress velocity factor; j is an exponent that accounts for non-linear velocity dependence of the plastic flow in the die entry; $\tau_0^{'}$ is the initial die-land wall shear stress as the paste velocity approaches zero; β is the die-land shear stress velocity factor, which accounts for the

increase of die-land wall shear stress with increasing paste flow velocity; and q is an exponent that accounts for non-linear velocity dependence of the shear flow in the die-land. It should be noted that $\sigma_0^{'}$, α, j, $\tau_0^{'}$, β, and q are not necessarily to be material parameters for the paste itself. Though the Benbow-Bridgwater equation provides a reasonably satisfactory prediction of ram extrusion data (mainly the relationship between the overall extrusion pressure drop and the mean paste flow velocity), for many semi-solid paste-like materials, such as ceramics and clays (Benbow et al 1991; Benbow and Bridgwater 1993; Blackburn and Bohm 1994; Chou et al 2003), it is basically a physically phenomenal model rather than a constitutive model for the ram extrusion process. This model can only give an overall description of paste flow in a ram extruder with simple symmetrical geometries, based on the assumption of simple rigid plastic or rigid-viscoplastic material behavior for the paste. The ram extrusion process of paste-like materials with elasto-viscoplastic constitutive behavior, in a non-axisymmetric geometry, is difficult to be directly described by the Benbow-Bridgwater model. In this case, only numerical methods might give a full description of the ram extrusion process of materials exhibiting complicated elasto-viscoplastic behavior.

In this study, a ram extrusion process of short fiber-reinforced, semi-solid, fresh cementitious composite, with a circular die entry and die-land, is investigated through experimental as well as numerical analysis. The extrusion load versus imposed ram displacement data, the evolution of deformation and distribution of various state variables within the paste flow are obtained through numerical simulation based on the ANSYS/LS-DYNA explicit finite element code, combined with an elasto-viscoplatic

constitutive model for the highly concentrated, short fiber reinforced fresh cementitious composite. Explicit analysis has been regarded as a more efficient solution than implicit analysis for large-deformation problems, such as materials forming process, like extrusion (Antunez 2000). The numerical procedure and the constitutive model are mainly verified quantitatively by comparing numerical and experimental results with respect to the extrusion load versus imposed ram displacement data. Then, the evolution of deformation and state variables within the composite during ram extrusion process is interpreted based on numerical results and ram extrusion mechanism. The effect of extrusion ratio, which is the ratio between the area of the barrel and that of the die-land, and extrusion velocity, which is ram driving velocity, on extrusion load is investigated based on experimental and numerical results. The aim of this research is to test the applicability of the numerical procedure, combined with the elasto-viscoplastic constitutive model, for describing ram extrusion process of short fiber-reinforced, semi-solid, fresh cementitious composite. The verified numerical procedure may also be used for modeling other forming processes for the fresh cementitious composite as well as for design and optimization of material processing equipment.

2. EXPERIMENTAL

The experiment program within the scope of this study is essentially divided into two parts. The first part involves rheological measurements to establish an appropriate constitutive model for the extrudable fresh cementitious composite, through orifice and

capillary extrusion (Zhou 2004; Zhou and Li 2005b) and upsetting tests (Zhou and Li 2006). The second part involves ram extrusion tests of the fresh cementitious composite under various extrusion conditions, i.e., extrusion ratios and/or extrusion velocities, that may appear in practice, from which the applied extrusion load with respect to the imposed ram displacement data are obtained. Both parts of the experiment program are carried out on the short fiber-reinforced fresh cementitious composite with the mix formulation shown in Table 1. The basic constitutive compositions include OPC (Ordinary Portland Cement) and slag with the weight ratio of 1:1 as the cementitious binder; 6mm-long PVA (Polyvinyl Alcohol) fiber with an average diameter of 14 μm, two types of silica sands (denoted as SS1 and SS2 with the nominal diameter of 300-600 μm and 90-150 μm, respectively) from David Ball Comp. Ltd with a weight ratio of 8:5 as aggregates, Methocel powder, produced by Dow Chemical Comp. Ltd, as the rheology enhancer and ADVA solution, made by W. R. Grace (HK) Ltd, as the superplasticiser. The water-to-binder weight ratio is 0.27 while the silica sands-to-binder weight ratio is 0.325. The dosage of ADVA solid powder is 0.375% of the weight of the binder and it is incorporated into the composite in the form of an aqueous solution with a concentration of 30% by weight as supplied by the manufacturer. The volume of PVA fiber is 2% of that of the readily mixed composite. It should be noted that the mix formulation, shown in Table 1, is a typical therapy for extrudable shore fiber-reinforced cementitious composite (Srinivasan et al 1999; Zhou and Li 2005a; Zhou and Li 2005b). To prepare the fresh cementitious composite for extrusion, cementitious binders (cement and slag), the fibers and the Methocel powder are first mixed for 3 minutes in a dry state at a low speed by a Hobart planetary mixer. Then water, with ADVA superplasticiser solution, is

added into the mixture and mixed for another 3 minutes. Once the dry powders are moistened, a higher speed is adjusted for 3-minutes high shear mixing till a dough-like paste is produced. This dough-like paste is then used for various experiments, including orifice extrusion, capillary extrusion, ram extrusion and upsetting tests referred in this study.

(Place Table 1 here)

It should be noted that short fiber-reinforced fresh cementitious composites for extrusion purpose are largely different from traditional cement paste, mortar, suspension, slurry, fresh self-compacting concrete and other fresh concrete which normally have larger water-to-binder ratio and better fluidity. The fresh cementitious composites for extrusion purpose are dough-like pastes, which exhibit almost no fluidity, but high cohesion and pseudo-plastic behavior under normal conditions (Srinivasan et al 1999; Zhou and Li 2005a; Li and Li 2007). Though a lot of extrusion practices have been successfully achieved, little research has been carried out on rheological behavior of the extrudable fresh cementitious composites and the extrusion process itself.

2.1 Material tests and rheological measurements

The experimental set-ups and procedures for orifice and capillary extrusion have been presented elsewhere (Zhou 2004; Zhou and Li 2005b) while those for upsetting tests have been reported in detail by Zhou and Li (2006). Based on these studies, the steady-state post-yield constitutive behavior of the extrudable short fiber-reinforced fresh cementitious composite has been formulated from which the shear flow stress, τ, is plotted as a function

of the plastic shear strain rate, $\dot{\gamma}^{vp}$. The post-yield shear flow behavior of the extrudable fresh cementitious composite has been found to be able to satisfactorily describe by the Herschel-Bulkley model (Zhou and Li 2005b) in the form of:

$$\tau = \tau_0 + k_{sc}(\dot{\gamma}^{vp})^m \qquad (2\text{-}1)$$

where τ_0 is the static shear yield stress, and k_{sc} and m are the shear plastic flow consistency and the shear flow index, respectively. The values of the material parameters in Eq. 2-1 have been obtained through orifice and capillary extrusion tests as $\tau_0 = 2.15\,kPa$, $k_{sc} = 4.17\,kPa \cdot S^m$ and $m = 0.38$ (Zhou 2004; Zhou and Li 2005b). Prior to yielding, the fresh cementitious composite exhibits elastic behavior with a constant Young's modulus of elasticity of $E = 8\,kPa$, which is obtained from its true stress versus true strain curve through upsetting tests presented elsewhere (Zhou and Li 2006).

(Place Fig. 2 here)

2.2 Ram extrusion

The experimental set-up and procedure for ram extrusion is similar to those described elsewhere (Zhou and Li 2005a), but different extrusion conditions are investigated in this research. The results of these ram extrusion tests are utilized to evaluate the applicability of the numerical procedure presented in this paper, combined with the elasto-viscoplastic constitutive model for the fresh cementitious composite, for describing its ram extrusion process. The experimental set-up for ram extrusion is shown in Fig. 2, where a home-made ram extruder, with smooth-surface stainless steel barrel and die, is mounted in a

servo-hydraulic Materials Test System (MTS) machine. Before extrusion, a certain amount of readily prepared, highly concentrated, dough-like fresh cementitious composite is fed into the barrel, with an inner diameter of 80 mm, of the extruder up to its brim. After this, ram extrusion test starts, and the paste inside the barrel is driven by the ram with a constant velocity till it flows out of the die exit in a steady state. Three sets of dies with diameters of 8 mm, 12 mm and 15 mm, respectively, are involved in experiment, resulting in three different extrusion ratios being 100, 44.4 and 28.4, respectively. The die-land lengths are truncated to obtain the die-land length-to-diameter ratio, L/D, being 0.83 and 4.79, respectively, for each set of dies. A series of tests with various extrusion velocities are conducted, representing a broad range of apparent strain rates imposed on the fresh composite. During extrusion, the data acquisition system records ram displacement, time and extrusion load. Each test is repeated three times and the average values are taken as the representative results. A typical experimental output on the variation of extrusion load with imposed ram displacement is shown in Fig. 3. In the initial stage when the ram pushes the fresh cementitious composite against the die-land, the composite undergoes upsetting which leads to a rapid increase in extrusion load until it attains a peak value (Point P in Fig. 3), where the paste breaks through the die exit. After this breakthrough, the extrusion load decreases, which is due to the reduction of the contact area, thus friction, between the composite and the barrel. The experimental data, after the breakthrough, clearly demonstrates the attainment of a steady state extrusion by a stable plateau value of extrusion load.

(Place Fig. 3 here)

3. NUMERICAL SIMULATION

3.1 Constitutive model and associated material parameters

A time-continuous model normally forms the basis for the constitutive equations in numerical simulations of elasto-viscoplastic material behavior (Lof and Boogaard 2001). In the time-continuous model, the relation between stress and strain, in both the elastic and the plastic domains, is usually defined in a rate formulation. Based on the infinitesimal deformation theory, it is reasonable to assume that the rate of deformation can be additively decomposed into an elastic (reversible) part and an inelastic (irreversible) part, so that the total strain rate, $\dot{\varepsilon}$, can be expressed as:

$$\dot{\varepsilon} = \dot{\varepsilon}^{el} + \dot{\varepsilon}^{vp} \tag{3-1}$$

where $\dot{\varepsilon}^{el}$ and $\dot{\varepsilon}^{vp}$ represent the elastic and viscoplastic strain rates, respectively. By assuming an isotropic material behavior, the elastic part is treated as being linear and is expressed in Cartesian index notation as:

$$\dot{\varepsilon}_{ij}^{el} = \frac{1+\nu}{E}\dot{S}_{ij} + \frac{1-2\nu}{3E}\dot{\sigma}_{kk}\,\delta_{ij} \tag{3-2}$$

Where E is the Young's modulus of elasticity, ν is the Poisson's ratio, $\dot{\sigma}$ is the rate of change of stress and $\dot{S}$ is the rate of change of deviatoric stress. A constant Poisson's ratio, $\nu = 0.465$, which is somewhat arbitrary, is incorporated in the constitutive model to represent a nearly incompressible material behavior, which have been found to be a reasonable assumption for this highly viscous paste-like material for extrusion purpose (Zhou 2004; Zhou and Li 2006).

For simplicity, it is further assumed that isotropic strain rate-hardening law is sufficient to describe the evolution of the flow stress of the extrudable fresh cementitious composite during plastic deformation. The strain rate-hardening law is formulated in terms of equivalent viscoplastic strain rate, $\dot{\bar{\varepsilon}}^{vp}$. Assuming an associative J_2 plastic flow where J_2 is the second invariant of the deviatoric stress tensor, the von Mises yield criterion is used to define the equivalent flow stress, $\bar{\sigma}$. Extending the notion of associative plasticity to viscoplasticity, the viscoplastic strain rate is assumed to be in the direction of the deviatoric stress, S, and is defined as

$$\dot{\varepsilon}^{vp} = \frac{3}{2}\dot{\bar{\varepsilon}}^{vp}\frac{S}{\bar{\sigma}} \tag{3-3}$$

where the equivalent viscoplastic strain rate, $\dot{\bar{\varepsilon}}^{vp}$, is defined as

$$\dot{\bar{\varepsilon}}^{vp} = \sqrt{\frac{2}{3}\dot{\varepsilon}^{vp} : \dot{\varepsilon}^{vp}} \tag{3-4}$$

and the equivalent flow stress, $\bar{\sigma}$, is calculated according to the von Mises yield criterion as

$$\bar{\sigma} = \sqrt{3J_2} = \sqrt{\frac{3}{2}S : S} \tag{3-5}$$

On the other hand, rate-dependent plasticity is often introduced by so-called overstress models, such as the Perzyna model (Perzyna 1967; Perzyna 1971; Wang et al. 1997; Lof et al. 2001; Ponthot 2002) or the Duvaut-Lions model (Simo and Hughes 1998). Contrary to the case of rate independent plasticity, in these models, the equivalent flow stress, $\bar{\sigma}$, is no longer constrained to remain less than or equal to the static yield stress, σ_0, but it could be greater than it. The part of the stress that is outside the static yield surface, which is called

overstress, determines the viscoplastic strain rate (Ponthot 2002). Clearly, an inelastic process can take place if, and only if, the overstress, $\mathrm{d} = \left\langle \bar{\sigma} - \sigma_0 \right\rangle$, is not less than zero, i.e. $\mathrm{d} \geq 0$, where $\langle \mathrm{x} \rangle$ denotes the MacAuley brackets defined by $\langle \mathrm{x} \rangle = 1/2(\mathrm{x} + |\mathrm{x}|)$. The classical viscoplastic models of the Perzyna (1966, 1971) type may be formulated as

$$\dot{\bar{\varepsilon}}^{vp} = D_{vp}\left(\frac{\bar{\sigma} - \sigma_0}{\sigma_0}\right)^{1/r} \tag{3-6}$$

where D_{vp} and r are the viscoplastic material parameters. Eq. 3-6 represents a mathematical relationship describing the evolution of the equivalent viscoplastic strain rate, $\dot{\bar{\varepsilon}}^{vp}$, as a function of the overstress, $\bar{\sigma} - \sigma_0$, in the plastic domain. The material parameters in Eq. 3-6, namely D_{vp} and r, can be obtained for the extrudable fresh cementitious composite through the following procedure.

First, the shear-form Herschel-Bulkley equation, i.e. Eq. 2-1, is transformed into its pertinent uniaxial formulation following the theoretical procedure proposed by Stouffer (1996) as

$$\bar{\sigma} = \sigma_0 + \mathrm{k}(\dot{\bar{\varepsilon}}^{vp})^{\mathrm{n}} \tag{3-7}$$

where the material parameters σ_0, k, and n are the uniaxial yield stress, the uniaxial plastic flow consistency and the uniaxial plastic flow index, respectively. On the other hand, for a material that obeys the von Mises yield criterion, the uniaxial form of the Herschel-Bulkley equation may be obtained from the graph of shear stress against shear strain rate by plotting

$\tau = \sigma / \sqrt{3}$ as a function of $\dot{\gamma}^{vp} = \sqrt{3}\,\dot{\varepsilon}^{vp}$ from its shear-form equation (Adams et al. 1997; Aydin et al. 2000). Substituting these relationships into Eq. 2-1 yields

$$\sigma = \sqrt{3}\tau_0 + (\sqrt{3})^{1+m} k_{sc} (\dot{\varepsilon}^{vp})^m \tag{3-8}$$

It has been found that the uniaxial bulk flow index, *n*, in Eq. 3-7 is approximately equal to the shear flow index, *m*, in Eq. 2-1, i.e. $n = m$, for the extrudable short fiber-reinforced fresh cementitious composite investigated in this study (Zhou 2004). In case of uniaxial bulk flow, $\bar{\sigma} = \sigma$ and $\dot{\bar{\varepsilon}}^{vp} = \dot{\varepsilon}^{vp}$. Therefore, by comparing Eqs. 3-7 and 3-8, the material parameters in Eq. 3-7 can be obtained as

$$\sigma_0 = \sqrt{3}\tau_0 \tag{3-9}$$

and

$$k = (\sqrt{3})^{1+m} k_{sc} \tag{3-10}$$

for the extrudable fresh cementitious composite. Rewriting Eq. 3-6 in the form of Eq. 3-7 gives

$$\bar{\sigma} = \sigma_0 + \left(\frac{\sigma_0}{D_{vp}^r}\right)(\dot{\bar{\varepsilon}}^{vp})^r \tag{3-11}$$

Thus, the interrelationships between the parameters in Eqs. 3-7 and 3-11 are obtained as $r = m$ and $D_{vp} = (\sigma_0 / k)^{1/m}$. Therefore, the associated material parameters in Eq. 3-11 are derived as $\bar{\sigma}_0$ = 3.72 kPa, D_{vp} = 0.101 S^{-1} and r = 0.38, by referring to the material test results of orifice extrusion and capillary extrusion presented elsewhere (Zhou 2004; Zhou and Li 2005b).

As may be seen from the above analysis, this elasto-viscoplastic constitutive model features the strain rate-dependent von Mises yield criterion, the associative flow rule and the nonlinear strain rate-hardening law. The rate-form constitutive model has been integrated into an incremental formulation and implemented into a numerical procedure based on the ANSYS/LS-DYNA explicit finite element code (Zhou 2004). In this paper, various ram extrusion processes are simulated by this numerical procedure, combined with the constitutive model for the short fiber-reinforced fresh cementitious composite for extrusion purpose.

(Place Fig. 4 here)

3.2 Geometries and the finite element model

In numerical analysis, the ram and the extruder, which is composed of the barrel and the die-land, are modeled as rigid objects. Due to axisymmetry, the deformation of the paste in the radial direction at the central of the extruder is zero. Thus, only a single azimuthal slice of the ram extruder and the cementitious composite inside from the centerline is modeled in numerical analysis with a two-dimensional (2-D) finite element model composed of a set of four-node isoparametric 2-D solid elements, which makes re-meshing easier. A typical initial mesh, generated by the ANSYS/LS-DYNA finite element code, is shown in Fig. 4 for the ram extrusion experimental set-up (see Fig. 2b) investigated in this study. A Coulombic friction criterion, with a constant static friction coefficient of μ=0.195 obtained through upsetting tests (Zhou and Li 2006), is adopted in the numerical procedure for simulating the

interaction between the deforming paste and the walls of the extruder. The interaction between the paste and the ram during extrusion is modeled in the same way as that between the paste and the platens in upsetting tests described elsewhere (Zhou and Li 2007). The fresh paste within the ram extruder is modeled by an Arbitrary Lagrangian-Eulerian (ALE) mesh as it travels through the die entry into the die-land, while the ram, the barrel and the die-land are modeled by a much coarser Lagrangian mesh to reduce computation time. The ALE mesh is very effective for simulating large deformation and large strain problems and it allows smoothing of a distorted mesh without requiring a complete re-meshing. Thus, it can largely avoid mesh distortion. A typical initial mesh for the highly concentrated fresh cementitious paste body in the barrel contains 1200-2000 elements, with the smallest element size being of order 10% of the radius of the die-land. In numerical simulation, an incremental analysis is performed, in which the imposed ram displacement during each analytical step, before re-meshing, is between 0.01 and 0.02% of the initial height of the fresh cementitious paste body in the barrel. A very small time step is adopted in numerical analysis to ensure stability in the fine mesh near the die entry, resulting in much longer computation time than that for the simulation of upsetting process presented elsewhere (Zhou and Li 2007). The computation time is even longer for cases with larger extrusion ratios than those with smaller extrusion ratios. In general, re-meshing is required to achieve a successful complete numerical simulation, resulting in that the element number keeps increasing during analysis. In this study, a series of ram extrusion processes of the fresh cementitious composite, under various extrusion velocities, die-land lengths and diameters, are simulated with the numerical procedure described above, combined with an elasto-viscoplastic constitutive model proposed

for the fresh cementitious composite tailored for extrusion purpose. The extrusion load can be obtained at any time during numerical analysis by integrating the longitudinal stress component, $\sigma_z(r)$, over the area of the ram. For an axisymmetric problem, the extrusion load, F_{ext}, is given by

$$F_{ext} = \int_0^{D_0/2} 2\pi r \sigma_z(r) dr \qquad (3\text{-}12)$$

where $\sigma_z(r)$ is the longitudinal stress of the elements contacting the ram. The extrusion load predicted at each deformation stage is then plotted against the imposed ram displacement to produce an extrusion load versus imposed displacement curve, to which the predicted extrusion load versus imposed displacement curve is referred in this paper. It is then compared with its experimental counterpart to test the applicability of the numerical procedure, combined with the constitutive model, to simulate ram extrusion process of the fresh cementitious composite.

(Place Fig. 5 here)

3.3 Comparison of numerical and experimental results

For every extrusion process, the numerical prediction is conducted from the start of extrusion until a steady state is reached. The relationship between extrusion load and the imposed ram displacement offers a channel for comparing the numerical and experimental results quantitatively. The numerical procedure, as well as the elasto-viscoplastic constitutive model for the fresh cementitious composite, presented in this study, is thus mainly verified by

this comparison. Figure 5 shows both the predicted and experimental extrusion load versus imposed displacement curves for the ram extrusion process through a 15 mm-diameter die, with a die-land length-to-diameter ratio of 0.83, at an extrusion velocity of 0.1 mm/s. It can be seen that the agreement, between the numerical and experimental results, is good during the upsetting stage and is within 5% difference under higher loads at steady-state extrusion. The predicted and experimental peak extrusion loads are 1485 N and 1562 N, respectively. In review of the uncertainty in the dynamic boundary interaction, the agreement between the predicted and experimental extrusion loads should be considered as satisfactory. Besides, the numerical prediction also indicates a decrease in extrusion load after the breakthrough, which is similar to that observed from experiment (as shown in Fig. 3). More results of the predicted and experimental extrusion load versus imposed ram displacement curves are shown in Figs. 6-8 for other ram extrusion processes. It can be seen from these figures that the results from numerical simulation are generally in good accordance with the pertinent experimental ones and the difference between the predicted and measured steady-state extrusion load is relatively low, which further verifies that the numerical procedure and the constitutive model, for the short fiber-reinforced fresh cementitious composite, presented in this paper can be used with confidence for the prescribed ram extrusion conditions.

(Place Figs. 6-8 here)

3.4 Interpretation of the paste flow in ram extrusion

Based on the verified numerical procedure, the evolution of deformation and distribution of various state variables, such as extrusion pressure and maximal principal stress, within the paste flow are also predicted throughout the extrusion process. The paste flow in ram extrusion is thus interpreted based on these numerical results, which also helps in validating the numerical procedure and the constitutive model for the fresh cementitious composite qualitatively and in understanding ram extrusion mechanism for the short fiber-reinforced fresh cementitious composite.

3.4.1 Evolution of deformation

At the initial stage of ram extrusion process when the ram pushes the fresh cementitious composite in the barrel, the composite paste commences upsetting. As the extrusion process continues, the paste flows towards the die-land where the velocity is the highest within the extruder. A breakthrough extrusion load (indicated by the peak Point 'P' in the extrusion load versus imposed displacement curve shown in Fig. 3) is necessary for the paste to be extruded out of the die exit. After reaching the peak extrusion load, the steady-state extrusion process starts, although the extrusion load decreases due to the decrease in friction between the paste and the walls of the barrel. As indicated by Figs. 5 to 8, the extrusion load reaches the peak value when the paste fulfills the die-land and starts to emerge, and then it decreases. The deformation of the composite along the extrusion direction (UY) are shown in Figs. 9a and b, for the ram extrusion process with a 30 mm-diameter die under a ram velocity of 0.1 mm/s, at ram imposed displacements of 1 mm and 4.2 mm, respectively. It can be seen that the

deformation of the composite in the die-land is significantly higher than that in the barrel, because of high extrusion ratio. In the corner between the die and the barrel, which is always referred as the static zone (see Fig. 9), the deformation of the composite is close to zero. The outline of the static zone, however, is not so obvious (see Fig. 9). When the composite travels in the die-land, a non-uniform displacement field occurs. It can be seen that the composite near the walls of the barrel and the die-land flows more slowly than the paste at the inner region, due to boundary friction existing between the composite paste and the walls of the extruder.

(Place Fig. 9 here)

3.4.2 Distribution of state variables within the paste flow

Distribution of extrusion pressure (SY), along the extrusion direction, is shown in Figs. 10a and b at the imposed ram displacements of 1 mm and 4.2 mm, respectively, for the ram extrusion process with a 30 mm-diameter die under a ram velocity of 0.1 mm/s. In general, negative stress could be found from these figures, which is representative of an essential compression-dominant state. However, tensile stress exists in the front surface of the paste flow, owing to the surface friction at the die-land wall, which restricts the paste flow. As a result, the front surface of the paste flow is mainly subjected to tension (see Figs. 10a and b). The distribution of the maximal principal stress (S1), shown in Fig. 11, provides a better indicator of stress state of the composite in ram extrusion, which implies that the front surface of the paste flow and the fresh cementitious composite near the die-land wall tend to be

subjected to tension along the extrusion direction. Tensile stress in the front surface of the paste flow is mainly due to two factors: first, the material in the inner region flows faster than that near the die-land wall; and second, the friction between the composite paste and the die-land wall which restricts the paste flow. It could also be ascribed to gravity as well. A common feature, observed from numerical results, is that there is a negative value of the maximum principal stress in the deformation zone and a positive value near the die-land wall and the front surface of the paste flow. The maximal principal stress increases from the top of the paste body in the barrel to the front surface of the paste flow in the die-land, changing gradually from compression to tension, which further confirms that the fresh cementitious composite, especially those near the die-land wall and at the front surface of the paste flow, tends to be subjected to tension in the extrusion direction when approaching the die exit.

(Place Fig. 10 and Fig. 11 here)

3.4.3 Effects of extrusion ratio and extrusion velocity

The effect of extrusion ratio on extrusion load is demonstrated in Fig. 12 for the extrusion processes with a 12 mm-diameter die and a 15 mm-diameter die, respectively, at the ram velocity of 0.2 mm/s. An increase in extrusion ratio, i.e., a decrease in die diameter, corresponds to an increase in apparent strain rate. Since the fresh cementitious composite is a strain rate-hardening material, its flow stress increases as strain rate increases. Thus more work is required to extrude the composite out of the die-land with smaller diameter than that with larger diameter, resulting in an increase in extrusion load. Besides, it can be seen from

Fig. 12 that the extrusion load increases more rapidly till reaching the steady-state value for the extrusion process with a higher extrusion ratio.

(Place Fig. 12 and Fig. 13 here)

The effect of extrusion velocity on extrusion load can be found from Fig. 13, in which both the numerical and experimental results are shown for the extrusion processes at extrusion velocities of 0.1 mm/s and 0.2 mm/s, respectively, with a die diameter of 12 mm and a die-land length-to-diameter ratio of 0.83. Again, since the fresh cementitious composite is a strain rate-hardening material, its flow stress increases as its strain rate increases. An increase of extrusion velocity results in an increase of apparent strain rate, thus equivalent flow stress, consequently, extrusion load as can be seen from Fig. 13 in which the extrusion load for the process under the extrusion velocity of 0.2 mm/s is much higher than that under the extrusion velocity of 0.1 mm/s. Again, the extrusion load in the former extrusion process increases more rapidly to a steady-state value than that for the latter.

4. CONCLUSIONS

A numerical procedure based on the explicit ANSYS/LS-DYNA finite element code, combined with an elasto-viscoplatic constitutive model for the extrudable fresh cementitious composite, has been established to simulate a series of ram extrusion processes. The predicted extrusion load versus imposed displacement data are compared with experimental results. The evolution of deformation and distribution of state variables within the composite paste flow in ram extrusion process are then interpreted based on numerical results and ram

extrusion mechanism. The effects of extrusion ratio and extrusion velocity on extrusion load are discussed. Based on experimental and numerical investigations, the main conclusions can be drawn as the following:

(1) The predicted extrusion load versus imposed displacement data agree reasonably well with experimental results for various extrusion processes, suggesting that the numerical procedure established and the constitutive model proposed for the fresh cementitious composite can be used with confidence for the prescribed ram extrusion processes. The extrusion load increases more rapidly to a steady-state value in case of a greater extrusion ratio and/or a higher ram velocity. In these processes, the steady-state extrusion loads are also greater.

(2) The evolution of deformation, as well as distribution of state variables within the paste flow, predicted by numerical analyses, gives promising interpretation of the fresh cementitious composite paste flow in various ram extrusion processes. Due to surface friction existing between the paste flow and the walls of the extruder, the paste in the central region moves faster than that along the extruder wall surface, resulting in that the composite at the front surface is mainly under tension, while the composite in other regions is mainly subjected to compression.

(3) The numerical procedure presented in this paper shows the potential for improving the understanding of the flow behavior of paste-like materials in extrusion, which might be applied to other forming processes for concentrated paste-like semi-solid elasto-viscoplastic materials.

Acknowledgement

The financial support from Hong Kong Research Grant Council under the contract of HKUST 6272/03E and China Ministry of Science and Technology under the grant of 2009CB32000 is gratefully acknowledged.

References

Adams, M. J., Aydin, I., Briscoe, B. J., and Sinha, S. K. (1997), "A Finite Element Analysis of the Squeeze Flow of An Elasto-viscoplastic Paste Materials," *Journal of Non-Newtonian Fluid Mechanics*, 71(1-2), 41-57.

Aldea, C., Marikunte, S., and Shah, S.P. (1998), "Extruded Fiber Reinforced Cement Pressure Pipes," *Advanced Cement Based Materials*, 8(2), 47-55.

Antunez, H. J. (2000), "Linear Elements for Metal-Forming Problems within the Flow Approach," *Computer Methods in Applied Mechanics and Engineering,* 190(5-7), 783-801.

Aydin, I., Biglari, F. R., Briscoe, B. J., Lawrence, C. J., and Adams, M., J. (2000), "Physical and Numerical Modelling of Ram Extrusion of Paste Materials: Conical Die Entry Case," *Computational Materials Science*, 18(2), 141-155.

Benbow, J. J., Jazayeri, S. H., and Bridgwater, J. (1991), "The Flow of Pastes through Dies of Complicated Geometry," *Powder Technology*, 65(1-3), 393-401.

Benbow, J. J. and Bridgwater, J. (1993), *Paste Flow and Extrusion*, Clarendon Press, Oxford.

Blackburn, S. and Bohm, H. (1994), "The Influence of Powder Packing on the Rheology of Fibre-Loaded Pastes," *Journal of Materials Science*, 29(16), 4157-4166.

Chou, S., Sydow, K., Martin, P. J., Bridgwater, J., and Wilson, D. I. (2003), "Stress Relaxation in the Extrusion of Paste," *Journal of European Ceramic Society*, 23(5), 637-646.

Li, Z. J., and Mu, B. (1998), "Application of Extrusion for Manufacture of Short Fiber Reinforced Cementitious Composite," *Journal of Materials in Civil Engineering*, 10(1), 2-4.

Li, Z. J., Mu, B., and Chui, S. N. C. (1999), "Systematic Study of Properties of Extrudates with Incorporated Metakaolin or Silica Fume," *ACI Materials Journal*, 96(5), 574-579.

Li, Z. J., Mu, B., and Chui, S. N. C. (2001), "Static and Dynamic Behavior of Extruded Sheets with Short Fibers," *Journal of Materials in Civil Engineering*, 13(4), 248-254.

Li, Zongjin, and Li, Xiangyu (2007), "Squeeze Flow of Viscoplastic Cement-Based Extrudate," *Journal of Engineering Mechanics*, ASCE, 133(9), 1003-1008.

Li, Zongjin, Zhou, Xiangming, and Shen, Bin (2004), "Fiber-Cement Extrudates with Perlite Subjected to High Temperatures," *Journal of Materials in Civil Engineering*, 16(3), 221-229.

Peled, A., and Shah, S. P. (2003), "Processing Effects in Cementitious Composites: Extrusion and Casting." *Journal of Materials in Civil Engineering*, 15(2), 192-199.

Lof, J., and Boogaard, A. H. Van Den (2001), "Adaptive Return Mapping Algorithms for J_2 Elasto-Viscoplastic Flow," *International Journal for Numerical Methods in Engineering*, 51(11), 1283-1298.

Perzyna, P. (1966), "Fundamental Problems in Viscoplasticity," In: Kuerti, G. (Eds.), *Advances in Applied Mechanics*, Academic Press: New York, 9, 243-377.

Perzyna, P. (1971), "Thermodynamic Theory of Plasticity," In Yih, C.-S. (Eds.), *Advances in Applied Mechanics*, Academic Press: New York, 11, 313-355.

Ponthot, J. P. (2002), "Unified Stress Update Algorithms for the Numerical Simulation of Large Deformation Elasto-Plastic and Elasto-Viscoplastic Processes," *International Journal of Plasticity*, 18(1), 91-126.

Simo, J. C., and Hughes, T. J. R. (1998), *Computational Inelasticity*, Springer-Verlag, 1998.

Shao, Y., Marikunte, S., and Shah, S. P. (1995), "Extruded Fiber-Reinforced Composites," *Concrete International*, 17(4), 48-52.

Shao, Y., and Shah, S. P. (1997), "Mechanical Properties of PVA Fiber Reinforced Cement Composites Fabricated by Extrusion Processing," *ACI Materials Journal*, 94(6), 555-564.

Srinivasan, R., DeFord, D., and Shah, S. P. (1999), "The Use of Extrusion Rheometry in the Development of Extruded Fiber-reinforced Cement Composites," *Concrete Science and Engineering*, 1(1), 26-36.

Stouffer, D. C., and Dame L. T. (1996), *Inelastic Deformation of Metals: Models, Mechanical Properties and Metallurgy*, John Wiley & Sons, New York.

Wang, W. M., Sluys L. J., and De Borst, R. (1997), "Viscoplasticity for Instabilities due to Strain Softening and Strain-rate Softening," *International Journal for Numerical Methods in Engineering*, 40(20), 3839-3864.

Zhou, Xiangming (2004), *Rheological Behaviors of the Fresh SFRCC Extrudate – Experimental, Theoretical and Numerical Investigations,* PhD Thesis, The Hong Kong University of Science and Technology, Hong Kong.

Zhou, Xiangming, and Li, Zongjin (2005a), "Characterization of Rheology of Fresh Fiber Reinforced Cementitious Composites through Ram Extrusion," *Materials and Structures*, RILEM, 38(275), 17-24.

Zhou, Xiangming, and Li, Zongjin (2005b), "Characterizing Rheology of Fresh Short Fiber Reinforced Cementitious Composite through Capillary Extrusion," *Journal of Materials in Civil Engineering*, ASCE, 17(1), 28-35.

Zhou, Xiangming, and Li, Zongjin (2006), "Upsetting Tests of Fresh Cementitious Composites for Extrusion," *Journal of Engineering Mechanics*, ASCE, 132(2), 149-157.

Zhou, Xiangming, and Li, Zongjin (2007), "Numerical Simulations of Upsetting Process of the Fresh Fiber-Cement Paste," *Journal of Engineering Mechanics*, ASCE, 133(11), 1192-1199.

APPENDIX I. Tables

Table 1 Mix formulation for the short fiber-reinforced fresh cementitious composite for extrusion purpose

Cement	Slag	SS1[a]	SS2[b]	PVA[c]	Methocel[d]	ADVA[e]	W/B[f]
0.5	0.5	0.2	0.125	2%	1%	0.375%	0.27

Note: SS1, SS2, Methocel, and ADVA are presented in weight ratio of binder;
PVA fiber is presented in the volume ratio of the paste;
[a]300-600 μm silica sand from David Ball Comp. (HK) Ltd;
[b]90-150 μm silica sand from David Ball Comp. (HK) Ltd;
[c]PVA = Polyvinyl Alcohol fiber;
[d]Methocel = rheology enhancing agent produced by Dow Chemical (USA);
[e]ADVA = superplasticiser made by W. R. Grace (HK) Ltd;
[f]W = water, B = binder (cement + slag)

APPENDIX II. Figures

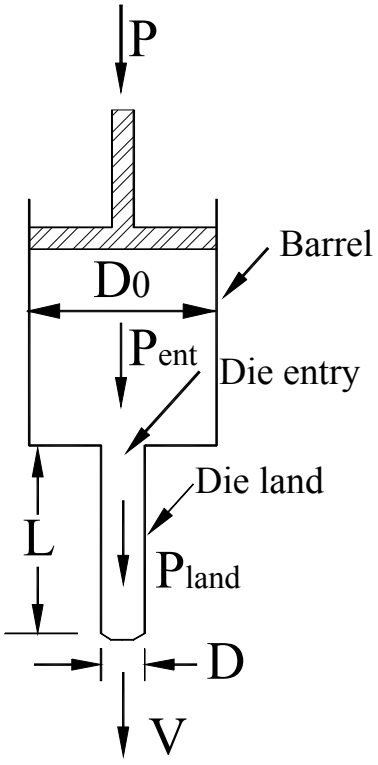

Fig. 1 Schematic diagram of Benbow-Bridgwater ram extrusion mechanism

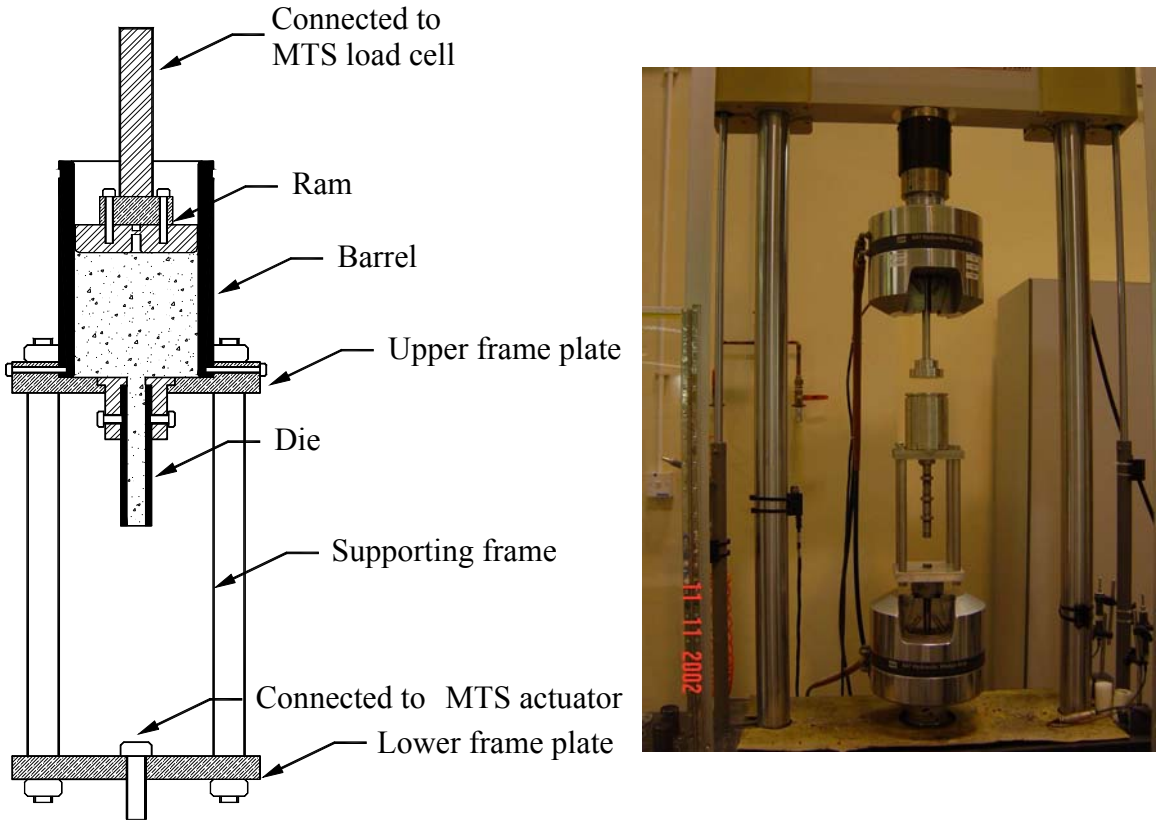

(a) Schematic diagram (b) Laboratory apparatus

Fig. 2 The experiment set-up of the ram extrusion test: (a) Schematic diagram; (b) Laboratory apparatus

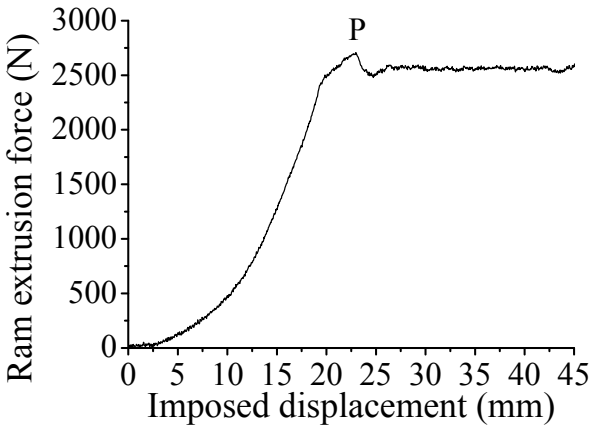

Fig.3 A typical ram extrusion load versus imposed displacement curve from experiment

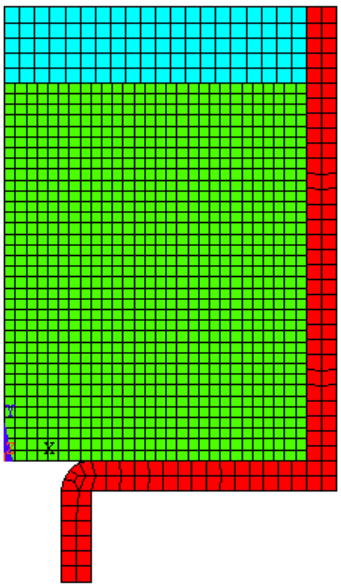

Fig. 4 The initial finite element mesh for simulating the ram extrusion process with a die diameter of 15 mm

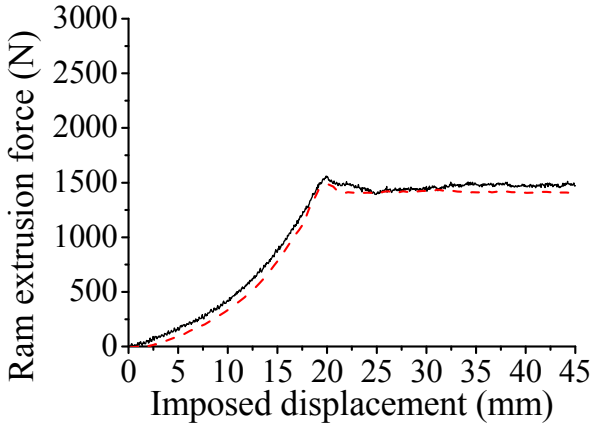

Fig. 5 The experimental (solid line) and predicted (dash line) extrusion load versus imposed displacement curves (D = 15 mm; L/D = 0.83 and V = 0.1 mm/s)

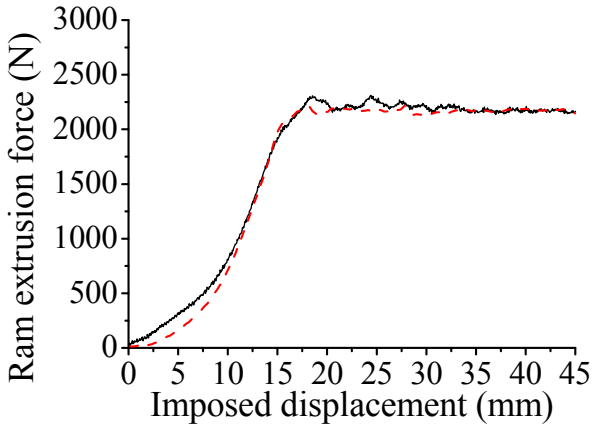

Fig. 6 The experimental (solid line) and predicted (dash line) extrusion load versus imposed displacement curves (D = 12 mm; L/D = 0.83 and V = 0.1 mm/s)

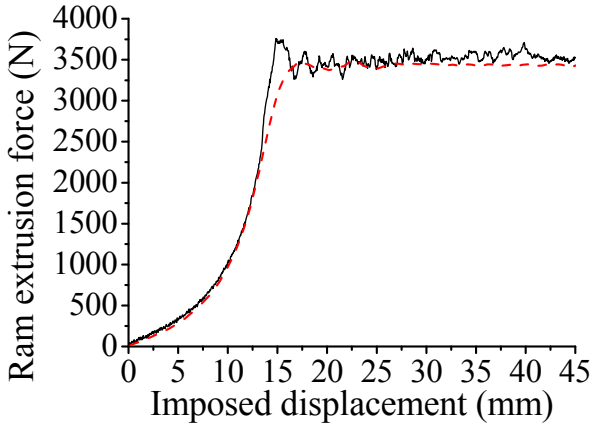

Fig. 7 The experimental (solid line) and predicted (dash line) extrusion load versus imposed displacement curves (D = 8 mm; L/D = 0.83 and V = 0.1 mm/s)

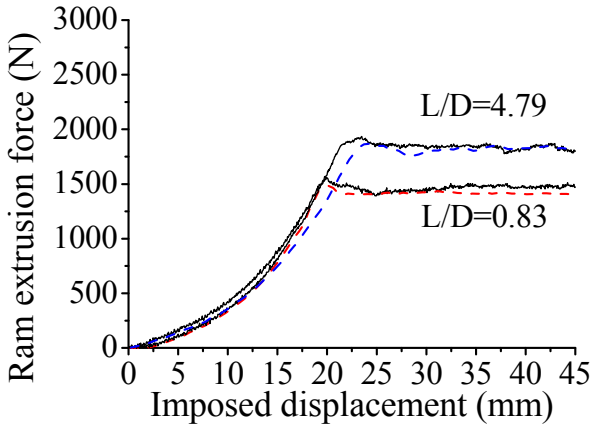

Fig. 8 The experimental (solid line) and predicted (dash line) extrusion load versus imposed displacement curves (D = 15 mm and V = 0.1 mm/s)

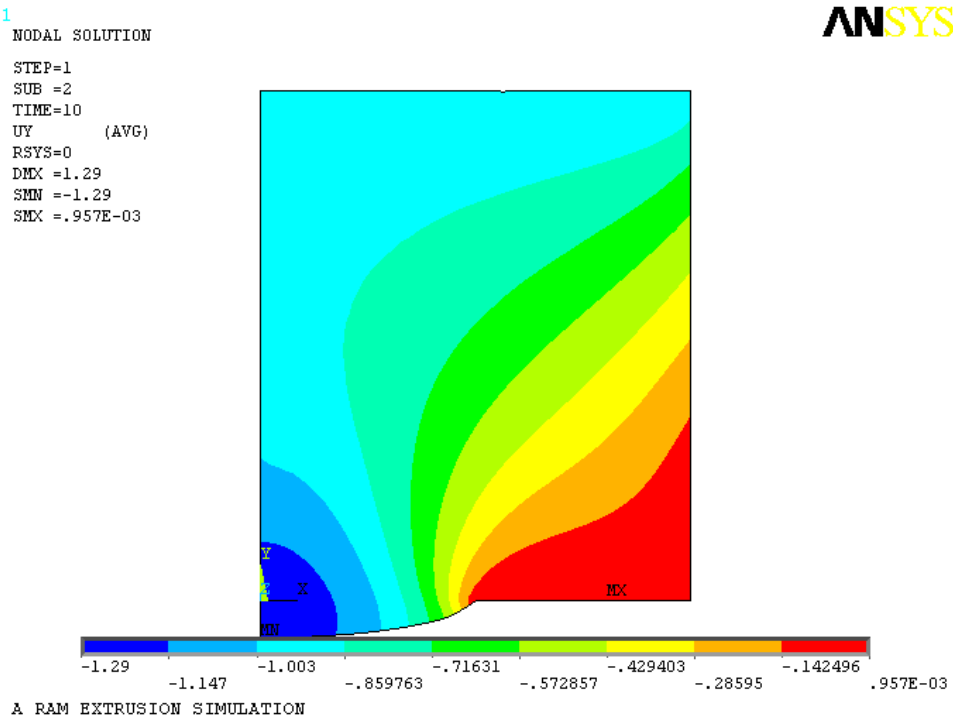

(a) At an imposed ram displacement of 1 mm

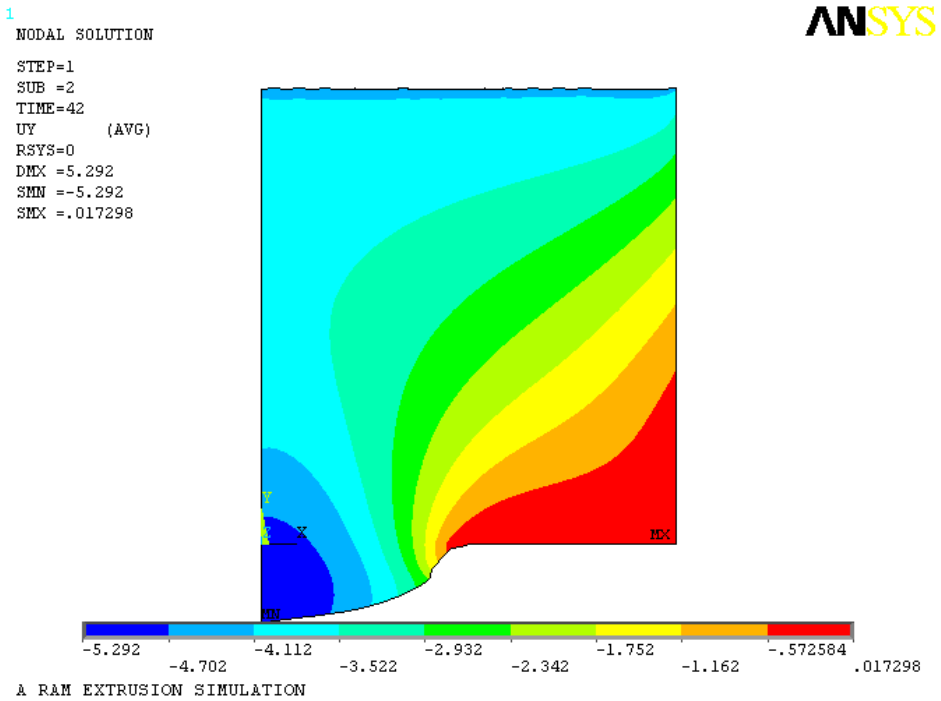

(b) At an imposed ram displacement of 4.2 mm

Fig. 9 The deformation (UY) of the fresh paste flow along the extrusion direction

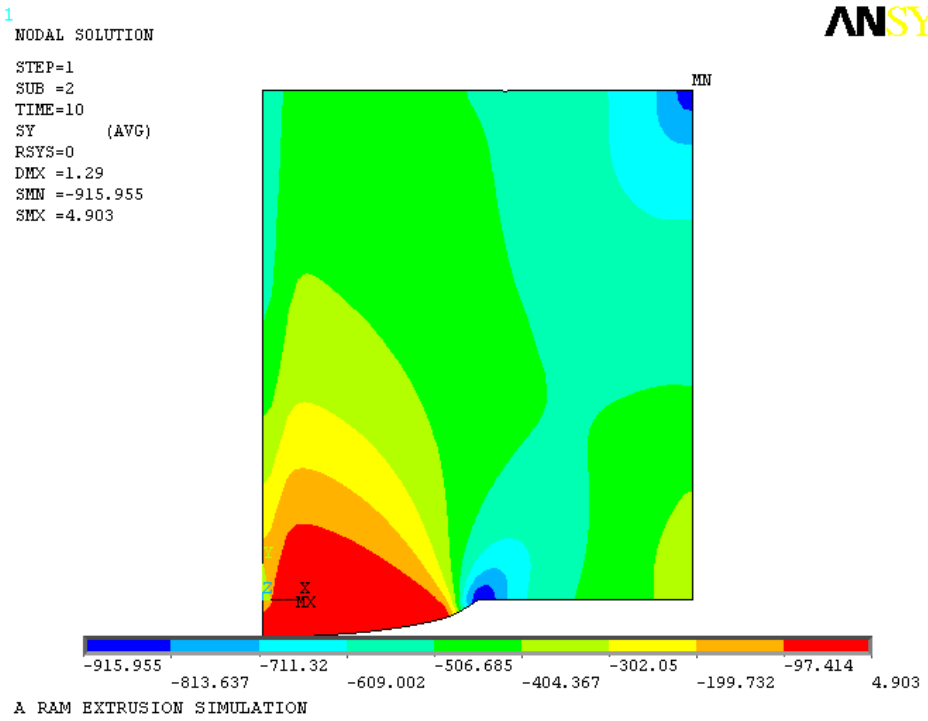

(a) At an imposed ram displacement of 1 mm

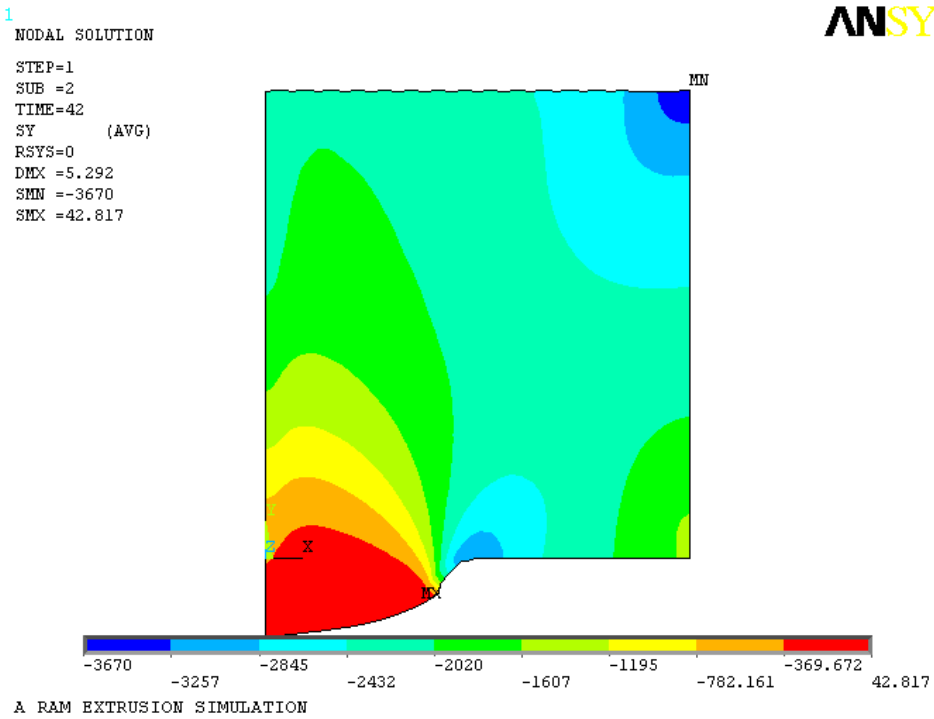

(b) At an imposed ram displacement of 4.2 mm

Fig. 10 The extrusion pressure (SY) within the paste flow along the extrusion direction

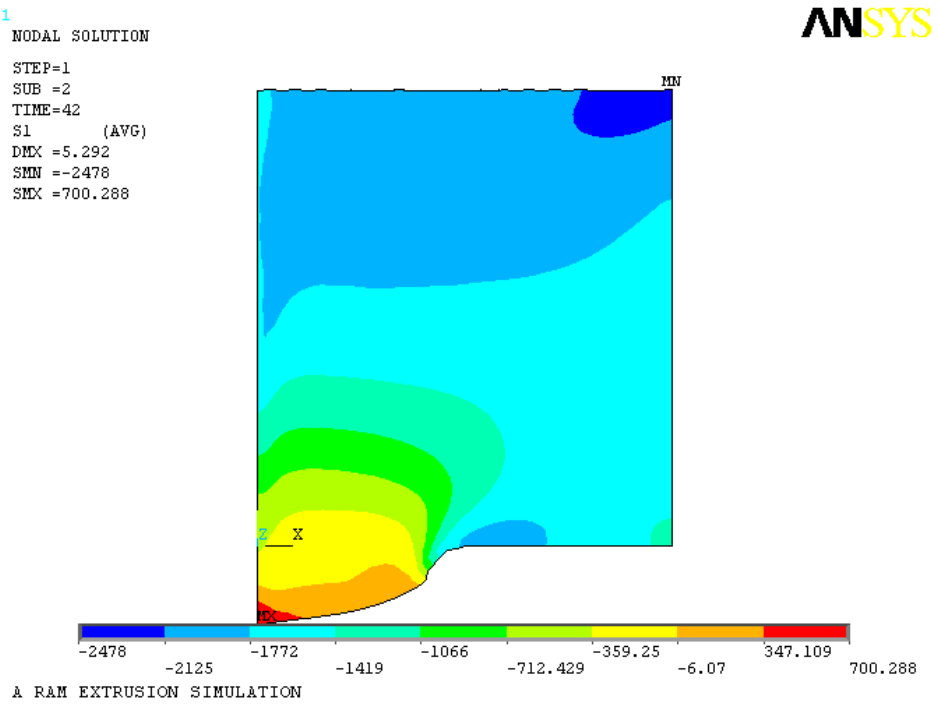

Fig. 11 The maximal principal stress (S1) within the paste flow at an imposed ram displacement of 4.2 mm

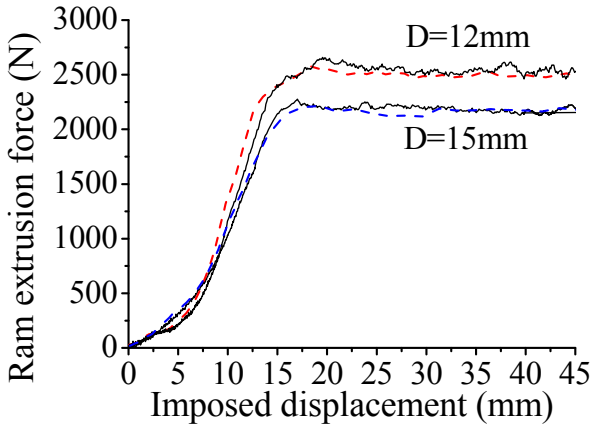

Fig. 12 The experimental (solid line) and predicted (dash line) extrusion load versus imposed ram displacement curves (L/D = 0.83 and V = 0.2 mm/s)

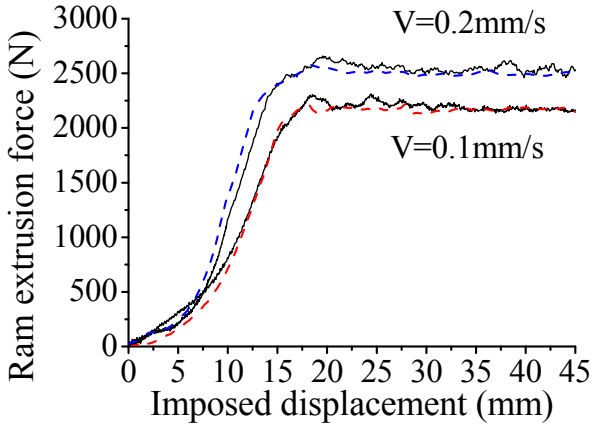

Fig. 13 The experimental (solid line) and predicted (dash line) extrusion load versus imposed ram displacement curves (D = 12 mm and L/D = 0.83)